

## Structure–Function Studies of PANDER, an Islet Specific Cytokine Inducing Cell Death of Insulin-Secreting $\beta$ Cells<sup>†</sup>

Jichun Yang, Zhiyong Gao, Claudia E. Robert, Brant R. Burkhardt, Helena Gaweska, Amary Wagner, Jianmei Wu, Scott R. Greene, Robert A. Young, and Bryan A. Wolf\*

*Department of Pathology and Laboratory Medicine, The Children's Hospital of Philadelphia and University of Pennsylvania School of Medicine, Philadelphia, Pennsylvania 19104*

*Received March 1, 2005; Revised Manuscript Received July 1, 2005*

**ABSTRACT:** PANDER (pancreatic derived factor, FAM3B) is a novel cytokine, present in insulin secretory granules, that induces apoptosis of  $\alpha$  and  $\beta$  cells of mouse, rat, and human islets in a dose- and time-dependent manner, and may be implicated in diabetes. PANDER has the predicted secondary structure of 4  $\alpha$ -helical bundles with an up–up–down–down topology, and two disulfide bonds. Eleven mutated PANDERs were constructed and expressed in  $\beta$ -TC3 cells to identify the essential region of PANDER involved in  $\beta$ -cell death.  $\beta$ -Cell function was assessed by assays of cell viability and insulin secretion. Based on quantitative real-time RT-PCR all mutant PANDERs had similar mRNA expression levels in  $\beta$ -TC3 cells. Immunoblotting showed that ten of eleven mutant PANDER proteins were synthesized and detected in  $\beta$ -TC3 cells. A mutant PANDER with no signal peptide, however, was not expressed. Truncation of helix D alone caused a 40–50% decrease in PANDER's activity, while truncation of both helices C and D resulted in a 75% loss of activity. In contrast, truncation of the N-terminus of PANDER (helix A, the loop between helices A and B, and the first two cysteines) had no effect on PANDER-induced  $\beta$ -cell death. The third and fourth cysteines of PANDER, C91 and C229, were shown to form one disulfide bond and be functionally important. Finally, the region between Cys91 and Phe152 constitutes the active part of PANDER, based on the demonstration that mutants with truncation of helix B or C caused decreased  $\beta$ -cell death and did not inhibit insulin secretion, as compared to wild-type PANDER. Hence, helices B and C and the second disulfide bond of PANDER are essential for PANDER-induced  $\beta$ -cell death.

Type 1 diabetes is characterized by an absolute insulin deficiency due to the chronic and progressive destruction of pancreatic  $\beta$ -cells mediated by the autoimmune system (1–4). Cytokines play a vital role in the destruction of pancreatic  $\beta$ -cells and the development of diabetes. In particular, interleukin-1 $\beta$  (IL-1 $\beta$ ),<sup>1</sup> as well as tumor necrosis factor- $\alpha$  (TNF- $\alpha$ ) and interferon- $\gamma$  (IFN- $\gamma$ ), has deleterious effects on  $\beta$  cells (5–9). In type 1 diabetes, macrophage and CD8+ T-cells are activated by IFN- $\gamma$  and IL-2 secreted from CD4+ T-cells. Activated macrophage and CD8+ cells secrete cytokines such as IL-1 $\beta$ , TNF- $\alpha$ , and IFN- $\gamma$ . These cytokines activate the apoptotic-signaling pathway by binding to their specific receptors on the membrane of pancreatic  $\beta$  cells, which results in lipid peroxidation, protein degradation and DNA damage, and finally insulinitis (10–14). More recently,

cytokines including TNF- $\alpha$ , leptin, and resistin have also been implicated in the development of insulin resistance and type 2 diabetes (15–19). Correlation studies between cytokines expressed in islets and autoimmune diabetes development in NOD mice and BB rats have demonstrated that  $\beta$ -cells' destructive insulinitis is associated with increased expression of T<sub>H</sub>1 (IFN- $\gamma$ , TNF- $\beta$ , IL-2, and IL-12) and proinflammatory cytokines (IL-1, TNF- $\alpha$ , and IFN- $\alpha$ ). IL-1 alone, or in synergy with IFN- $\gamma$ /TNF- $\alpha$ , causes nitric oxide (NO) synthesis, necrosis, and apoptosis of pancreatic  $\beta$ -cells of mice, rat, and human islets (6, 13, 20, 21). Transgenic expression of IFN- $\alpha$  or IFN- $\gamma$  within the pancreatic islets results in increased insulinitis and diabetes. Similarly, transgenic expression of TNF- $\alpha$  within the pancreatic islets also induces insulinitis, although it does not result in diabetes (22–24). These results suggest that the local production of cytokines has a distinct role in the development of insulinitis and subsequent  $\beta$ -cell destruction, which results in type-1 diabetes.

PANDER (pancreatic derived factor, FAM3B) is a newly discovered protein that was identified by a database search for novel cytokines with the predicted secondary structure of 4  $\alpha$ -helical bundles with an up–up–down–down topology (25). Because the secondary structure of cytokines is highly conserved through evolution unlike the amino acid sequence, this strategy, based on the ostensible recognition of folds algorithm (25), was expected to yield novel cytokine-like proteins. PANDER is a 235-amino acid protein with a secretion signal peptide (amino acids 1–29), and four

<sup>†</sup> This work was supported by grants from the Juvenile Diabetes Research Foundation (to J.Y. and B.A.W.) and the National Institutes of Health, DK49814 (to B.A.W.), and T32-DK07314-23 (to B.R.B.) from the NIDDK, National Institutes of Health. The Radioimmunoassay Core of the Institute of Diabetes, Obesity and Metabolism of the University of Pennsylvania is supported by NIH Grant DK 19525.

\* Author to whom correspondence should be addressed. Mailing address: Department of Pathology and Laboratory Medicine, Children's Hospital of Philadelphia, 5135 Main Bldg, 34th St. and Civic Center Blvd., Philadelphia, PA 19104-4399. Tel: (215) 590-2869. Fax: (215) 590-1021. E-mail: wolfb@mail.med.upenn.edu.

<sup>1</sup> Abbreviations: IL-1 $\beta$ , interleukin-1 $\beta$ ; IL-6, interleukin-6; TNF- $\alpha$ , tumor necrosis factor- $\alpha$ ; IFN- $\gamma$ , interferon- $\gamma$ ; PANDER, pancreatic derived factor or FAM3B; Wt, wild-type; aa, amino acid; Ad, adenovirus; FBS, fetal bovine serum; KRB, Krebs Ringer bicarbonate buffer.

Table 1: Mutants of Mouse PANDER

mutant name	amino acids truncated	amino acid mutated or inserted
M1	177–235 (Helix D)	
M2	177–235	mutation Ser176 to Cys176
M3	138–235 (helices C, D)	
M4	138–235	insertion Cys138
M5	31–90 (helix A)	
M6	31–90	mutation Cys91 to Ser91
M7	31–112 (helices A, B)	
M8	31–112	mutation Val113 to Cys113
M9	93–112 (helix B)	
M10	1–29 (the signal peptide)	insertion ATG before helix A
M11	none	mutation C229 to S229

cysteines (C61, C69, C91, and C229) (26). Modeling study indicates that the four cysteines probably form two disulfide bonds, but the importance of these bonds to the biological functions of PANDER is unknown. Recombinant PANDER prepared in *Pichia pastoris* is a mixture of PANDER fragments cleaved at residues Ser46 and Ala55 with a mass of 21.1 kDa and 20.0 kDa, respectively (26). Our previous studies showed that recombinant PANDER induces apoptosis of  $\alpha$  and  $\beta$  cells of mouse, rat, and human islets in a dose- and time-dependent manner (27). Our studies also showed that adenoviral overexpression of full-length PANDER in  $\beta$ -cells has potent cytotoxic effects on cell viability of mouse islets (28). The mechanisms of PANDER-induced apoptosis are unknown, and the PANDER receptor has not been identified to date. Identification of the PANDER receptor would be an important goal to understand the physiological function of PANDER in addition to its documented apoptotic effects on  $\beta$ -cells. The structure–function relationship of PANDER is also unknown. The aim of this study is to identify the essential domain of PANDER by analyzing the relative activities of a series of truncated and mutated PANDER analogues (Table 1), in comparison to that of wild-type PANDER. We anticipate that the structure–function studies will provide useful information for the identification of PANDER's receptor.

## MATERIALS AND METHODS

**Construction of Mutant PANDER Plasmids and Adenoviruses.** Prior to mutagenesis, the wild-type mouse PANDER cDNA (670 bp) (26) was cloned into 4.1 kb pShuttle plasmid (BD Biosciences), which contains a CMV promoter, *ApaI* and *NotI* restriction enzymes sites and is kanamycin resistant, creating wild-type PANDER plasmid (Wt-PAN). Wt-PAN was used as a template for all PANDER mutant constructions. PCR primers with the desired mutation were synthesized. All PCR reactions were done with QuickChange Multi Site-Directed Mutagenesis Kit (Stratagene) with the following conditions: 95 °C (1 min), followed by 30 cycles of 95 °C (1 min), and 55 °C (1 min), and 65 °C for 10 min (2 min/kb plasmid length). When the PCR reaction was completed, the methylated template was completely digested by *DpnI* and the single mutant strand was added to ultracompetent *Escherichia coli*. The transformed cells were plated on LB plate containing 50  $\mu$ g/mL kanamycin and incubated at 37 °C overnight. Positive clones were first identified by the predicted molecular weights of plasmid digestion products using restriction enzymes *ApaI* and *NotI*, followed by DNA sequencing for definitive confirmation.

For truncation of C-terminal regions, a stop codon was engineered just before the region to be truncated. Because the fourth cysteine, C229, is at the far C-terminus of PANDER, truncation of the C-terminus will damage the putative disulfide bond involving C229. To address this, we created another mutant with C-terminus truncated but added a cysteine before the stop codon, to preserve the disulfide bond.

For truncation of the N-terminus without losing the signal peptide (aa1–29), we connected the signal peptide to the new N-terminus of the truncated PANDER analogues. In brief, wild-type PANDER was first mutated to introduce *BlnI* recognition sites at both ends of the region to be deleted. Introduction of the *BlnI* site resulted in the addition of two amino acids (Pro-Arg) between the signal peptide and the new N-terminus. The plasmid was then digested with *BlnI*. The two fragments were separated, and the long fragment was purified and religated end-to-end. If the truncation caused the loss of a cysteine and thus a disulfide bond, another mutant PANDER was also created by adding a new cysteine as described above.

To construct pShuttle containing eGFP gene, eGFP cDNA was cut out from the plasmid pEGFP-1 with *ApaI* and *NotI* and then cloned into the pShuttle with the same enzymes. For large-scale preparation of plasmids needed for cell transfection, the plasmid was proliferated in *E. coli* and purified using Endo-free Plasmid Maxi Kit (QIAGEN Inc). The DNA was precisely quantified by ultraviolet absorbance before transfection.

The mutant PANDER adenoviruses were constructed at The Vector Core of University of Pennsylvania.

**Transfection of  $\beta$ -TC3 Cells with Wt and Mutant PANDER Plasmids.**  $\beta$ -TC3 cells ( $1.5\text{--}2.0 \times 10^5$ ) (passages 40–50) were seeded in each well of a 24-well plate with 0.5 mL of antibiotic-free RPMI 1640 (11 mM glucose and 10% FBS) 1 day before transfection. For transfection, 0.8  $\mu$ g plasmid was diluted into 50  $\mu$ L of prewarmed Opti-MEM medium (antibiotic and serum free) and mixed gently. At the same time, 2  $\mu$ L of Lipofectamine 2000 (Invitrogen) was prediluted into 50  $\mu$ L of Opti-MEM medium. The diluted DNA and Lipofectamine 2000 mixtures were preincubated at room temperature for 5 min and then combined to generate the DNA–Lipofectamine 2000 complex (room temperature, 20 min). After incubation, the DNA–Lipofectamine 2000 complex (100  $\mu$ L) was added to the cultured cells (total transfection volume is 600  $\mu$ L). The plate was rocked back and forth gently and then incubated at 37 °C in 5% CO<sub>2</sub> for 4 h. After incubation, the transfection medium was replaced with 1 mL of RPMI 1640 (3 mM glucose and 1% FBS); the

cells were then cultured at 37 °C in 5% CO<sub>2</sub> until further experiments. In some experiments,  $3 \times 10^5$   $\beta$ -TC3 cells in suspension were seeded 30 min before transfection, which was performed as described above.

**Infection of  $\beta$ -TC3 Cells with PANDER Adenoviruses.** One day before infection,  $3 \times 10^5$  cells were seeded in 24-well plate in 1 mL of normal RPMI 1640 (10% FBS, 11 mM glucose). Before infection, the cells were washed twice with 1 mL of serum-free RPMI 1640 before 250  $\mu$ L of serum-free medium was added. The virus particles were added to the wells to reach the indicated number of particles/cell. The plate was incubated at 37 °C in 5% CO<sub>2</sub> for 3 h. After incubation, cells were washed once with normal RPMI 1640 and then cultured in 1 mL of RPMI 1640 (1% FBS, 3 mM glucose) until further experiments.

**Confirmation of Overexpression by Quantitative RT-PCR.** To compare the relative effectiveness of Wt and mutant PANDERs, it is important to overexpress them at the same level. Quantitative RT-PCR was used to detect the transfection and expression efficiency at the mRNA level. Since it is technically impossible to analyze all the mutant PANDER mRNA with one set of PCR primers, the following set of primers, which match the 470–519 region of wild-type PANDER, was used. It allowed the comparison of overexpression levels for M1-PANDER and M2-PANDER, representing the C-terminus truncations, and M5-PANDER and M6-PANDER, representing N-terminus truncation. The primer sequences are as follows: forward, 5'-TCC CTG CTG TTC ATG GTG ACT-3'; reverse, 5'-GGC TTC TAT GGC ATC CTT TGC-3'; probe, 5'/56-FAM/ATG ATG ATG GAA GTT CCA AAC TGA AGG CTC A/36-TAMTph/3'.

Forty-eight hours after transfection, the cells were washed twice with 1 mL of ice-cold PBS. Total RNA was extracted using RNeasy Mini Kit (QIAGEN Inc.) with DNA-free protocol. Agarose gel electrophoresis was used to analyze the quality of total RNA before RT-PCR assay. Real-time RT-PCR was performed with Universal PCR Master Mix Kit (TaqMan) using 200 ng of total RNA in each reaction. The RT-PCR procedure was the following: 95 °C for 10 min, followed by 50 cycles of 95 °C for 15 s, 60 °C for 1 min. Quantitative values were obtained as threshold PCR cycle number (Ct) when the increase in fluorescent signal of PCR product became an exponential growth. Target gene mRNA level was normalized to that of  $\beta$ -actin in the same sample. In brief, the relative expression level of the target gene compared to that of  $\beta$ -actin was calculated as  $2^{-\Delta Ct}$ , where  $\Delta Ct = Ct_{\text{target gene}} - Ct_{\beta\text{-actin}}$ . The ratio of relative expression of the target gene in treated cells to that of control cells was then calculated as  $2^{-\Delta\Delta Ct}$ , where  $\Delta\Delta Ct = \Delta Ct_{\text{treated cells}} - \Delta Ct_{\text{control cells}}$  (8, 29, 30). Each sample was measured in duplicate in each experiment. When the  $\beta$ -actin levels were similar in all the samples, the target gene levels were compared directly using the Ct value difference among the experimental groups.

**Western Blot Assays.** Cells were seeded and transfected in 12-well plates and cultured for 48 h. The cells were washed twice with 1 mL of ice-cold PBS, before adding 250  $\mu$ L/well fresh Roth lysis buffer (50 mM HEPES, 150 mM NaCl, 1% Triton X-100, 5 mM EDTA, 5 mM EGTA, 20 mM Na pyrophosphate, 20 mM NaF, 0.2 mg/mL PMSF, 0.01 mg/mL leupeptin, and 0.01 mg/mL aprotinin, pH 7.4). The cells were dissolved in lysis buffer by scraping and pipetting

on ice. The lysate was transferred to a 1.5 mL tube and centrifuged at 4 °C at 13 000 rpm for 10 min. The protein concentration in the supernatant was determined by bicinchoninic acid assay to equalize the amount of protein in all conditions. SDS loading buffer was added to samples in a ratio of 1:4 before samples were boiled for 6 min, and analyzed by SDS-PAGE. Electrophoresis was performed at 170 V. Proteins in the gel were transferred to the Hybond-C Extra membrane (Amersham Biosciences) at 120 V for 2 h at 4 °C. The membrane was washed once with 10 mL of 1xTBST (1.2 g/L Tris Base, 5.84 g/L NaCl, 0.1% Tween-20, pH 7.5) before blocking in 20 mL of blocking buffer (1xTBST containing 1% BSA) at room temperature for 1 h. The membrane was incubated in 1:1000 rabbit anti-PANDER polyclonal antibody at 4 °C overnight. The membrane was washed five times with 15 mL of 1xTBST, incubated in 1:5000 peroxidase-conjugated donkey anti-rabbit antibodies at room temperature for 1 h before washing as above, and then developed with ECL.

**MTT Assay of Cell Viability.** The assay is based on the ability of viable cells to reduce MTT (*C,N*-diphenyl-4,5-dimethyl thiazol-2-yl tetrazolium bromide) to insoluble colored formazan crystals as described previously (31).  $\beta$ -TC3 cells were transfected with truncated PANDER plasmids as described above. Plasmid pShuttle containing wild-type PANDER and pShuttle vehicle were used as positive and negative control. Forty-eight hours after transfection, the cells were washed twice with 1 mL of prewarmed KRB. Cells were then incubated at 37 °C in 5% CO<sub>2</sub> for 1 h in 1 mL of KRB containing 20 mM glucose and 0.5 mg/mL MTT. The supernatant was aspirated, and 0.5 mL/well 2-propanol was added. The plate was incubated at room temperature in darkness for 1 h to completely dissolve formazan crystals. The absorbance was measured at 560 nm using Wallac 1420 Multilabel Counter (PerkinElmer Life Sciences, Gaithersburg, MD). All the data were normalized to control (transfected with pShuttle vehicle). The relative activity of truncated PANDERs to wild-type PANDER was calculated by the following formula: relative activity (%) = (control – PANDERs)/(control – wild type)  $\times$  100%, control = 100%, PANDERs and wild-type stand for the normalized cell viability value of truncated PANDERs and wild-type PANDER, respectively.

**Live/Dead Assay Using Calcein-AM/EthD-1.** A two-color fluorescence cell viability assay was used based on the ability of calcein-AM to be retained within the live cells, inducing an intense uniform green fluorescence and ethidium homodimer (EthD-1) to bind the nuclei of damaged cells (31). In brief, 48 h after transfection of attached cells, the medium was aspirated and the cells were washed twice with 0.5 mL of prewarmed sterile PBS. The washing solutions were collected together and centrifuged, and then the supernatant was discarded. The pellet was resuspended in 200  $\mu$ L of PBS containing 10 nM calcein-AM and 4  $\mu$ M EthD-1. This resuspended solution was then added into the corresponding well, and the plate was incubated at room temperature in darkness for 45 min. The green fluorescence of the live cells was measured using a Wallac 1420 multilabel counter (PerkinElmer Life Sciences, Gaithersburg, MD). Excitation was at 488 nm, and emission was detected at 510 nm with a band-pass filter. Images of the stained cells were captured by digital camera controlled by SimplePCI software (31).



**Insulin Release and Acute Secretion Assays.** For insulin release assay, the medium was collected 48 h after transfection and centrifuged at 13 000 rpm at 4 °C for 10 min. The supernatant was submitted to the Radioimmunoassay Core of the Institute of Diabetes, Obesity and Metabolism of the University of Pennsylvania for insulin content analysis. For acute insulin secretion, the transfected cells were cultured for 48 h. The cells were washed twice with KRB-G0 and preincubated in 0 mM glucose for 1 h, then challenged with 20 mM glucose for 1 h. The insulin secretion in the medium was measured as above.

**Detection of Secreted PANDER in the Medium of Transfected  $\beta$ -TC3 Cells.** The cells were transfected in 12-well plates and cultured for 48 h under various experimental conditions. The medium was collected and centrifuged at 13 000 rpm at 4 °C for 10 min. The pellet was discarded, and ammonium sulfate was added to the supernatant (500 mg/mL of medium). After careful mixing, the solution was incubated at 4 °C for 1 h and then centrifuged at 4 °C at 13 000 rpm for 25 min. The pellet was resuspended in water and analyzed for PANDER content by immunoblotting.

**Statistical Analysis.** Data are presented as mean  $\pm$  SEM. Statistical significance of differences between groups was analyzed by unpaired Student's *t* test or by one-way analysis of variance (ANOVA) when more than two groups were compared.

## RESULTS

**Construction and Overexpression of Wild-Type and Mutant PANDERs in  $\beta$ -TC3 Cells.** To identify the essential regions of PANDER, a series of truncated PANDER mutants were constructed and cloned into the expression vector pShuttle, which contains a CMV promoter. To truncate the C-terminus, we introduced a stop codon before the region to be deleted. To truncate the N-terminus, the entire signal peptide (amino acids 1–29) was kept, since it is expected to be required for intracellular PANDER processing (Figure 1). Mutant PANDER proteins were expressed in  $\beta$ -TC3 cells followed by assessment of insulin secretion and cell death. To demonstrate that all mutant PANDERs had similar expression levels in  $\beta$ -TC3 cells, mRNA levels were measured by quantitative RT-PCR. The Ct value was reduced from  $27.8 \pm 1.0$  in control cells transfected with pShuttle vector to  $16.8 \pm 0.6$  in wild-type transfected cells, corresponding to a 2048-fold increase of PANDER mRNA. There was no significant difference in Ct values among Wt, M1, M2, M5, and M6 mutants (Figure 2A). Cells transfected with Wt, M1, M2, M5, and M6 also had similar  $\beta$ -actin Ct levels as control (Figure 2B). These results indicate that the Wt, M1, M2, M5, and M6 plasmids resulted in similar expression levels. pShuttle-EGFP was used to determine the efficiency of transfection, which was 20–30% in attached  $\beta$ -TC3 cells and 30–40% in cells in suspension (Figure 2C).

Immunohistochemistry showed that similar expression levels of the M1, M2, M5, and M6 mutants were obtained compared to wild-type expression levels (data not shown). Immunoblotting showed that 10 of 11 mutant PANDER proteins were synthesized in  $\beta$ -TC3 cells. The molecular weight of full-length Wt PANDER is about 26 kDa (235 aa). The actual mass of M1 (175 aa), M2 (175 aa), M3 (138 aa), and M4 (138 aa) closely matched the predicted mass

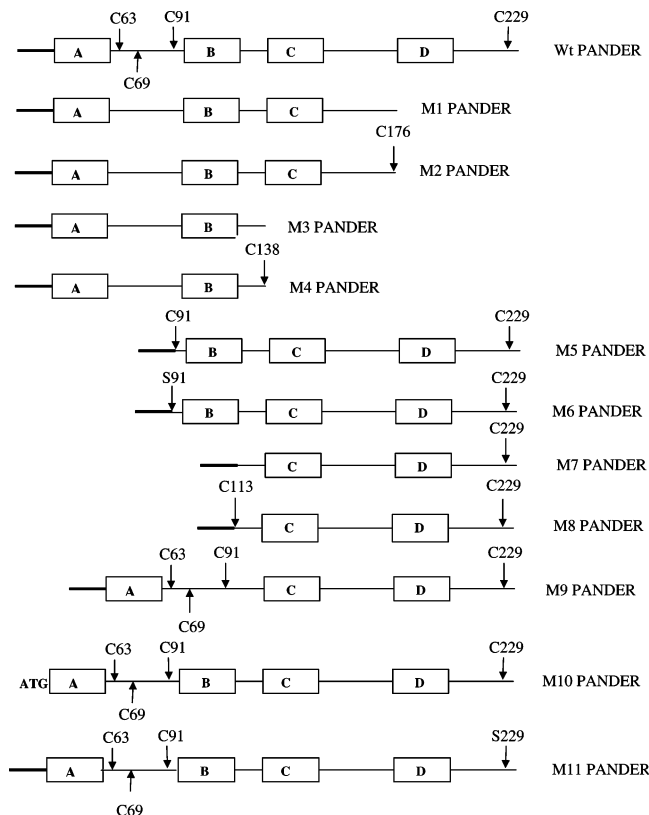


FIGURE 1: Design of PANDER mutants. The signal peptide of wild-type PANDER is shown in bold, while the four helices are indicated by the letters A, B, C, and D. C63, C69, C91, and C229 are the four cysteines in wild-type PANDER. Wt, wild-type; M, mutant.

(about 19, 19, 15, and 15 kDa, respectively, Figure 3A). The actual molecular weights of M5 (176 aa), M6 (176 aa), M7 (154 aa), M8 (154 aa), and M9 (217 aa) were about 19, 19, 17, 17, and 24 kDa, respectively (Figure 3B). M11 (235 aa) has a molecular weight similar to that of Wt PANDER (Figure 3C). The results also indicated that the polyclonal antibody recognized the wild-type PANDER with the highest affinity and recognized the mutant PANDERs with lower affinities. These differences are presumably due to the loss of antigen epitopes in mutant PANDERs (Figure 3A,B), which was supported by the observations that the polyclonal antibody recognized the mutant PANDERs with a similar amino acid sequence by the similar affinity (Wt and M11, M1 and M2, M3 and M4, M5 and M6, M7 and M8) (Figure 3). This also further confirmed the real-time RT-PCR data that all mutant PANDERs have similar transfection and expression efficiency in the present study (Figures 2 and 3).

**Effect of C-Terminal and N-Terminal Mutation on PANDER Activity.** M1 mutant PANDER maintained  $55 \pm 13\%$  ( $p < 0.05$ ) of Wt PANDER cytotoxic activity, while M2 maintained  $68 \pm 5\%$  (Figure 4A,B). When compared to M1 with Ser176, more activity was maintained in M2 with Cys176, indicating that mutation of Ser176 to Cys176 had restored some activity. This implies that Cys229 (deleted in M1) in wild type is probably involved in formation of a disulfide bond. M3 and M4 maintained about  $25 \pm 7\%$  and  $31 \pm 9\%$  of Wt PANDER activity (Figure 4A,B), respectively. Significant decrease of activity was observed in M3 and M4 when compared to M1 and M2, indicating that truncation of helix C affects the conformation of PANDER and its activity. It is interesting that M5 maintained almost

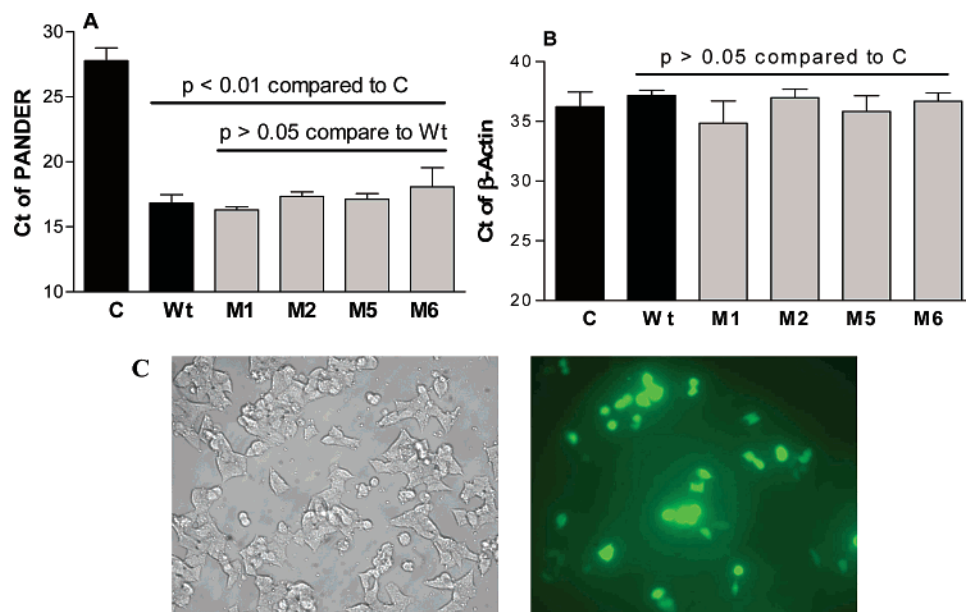


FIGURE 2: Expression efficiency of PANDER mutants in  $\beta$ -TC3 cells. One day before transfection,  $3.0\text{--}4.0 \times 10^5$   $\beta$ -TC3 cells were seeded per well as described in Materials and Methods. Cells were transfected with control (C) plasmid, wild-type (Wt) or mutant PANDERS (M1 to M6). Forty-eight h later, total RNA was extracted, and PANDER mRNA levels were determined by quantitative real-time RT-PCR using  $\beta$  actin as control. (A) Real-time PCR of PANDER. (B) Real-time PCR of  $\beta$  actin. (C)  $\beta$ -TC3 cells transfected with pShuttle-eGFP and analyzed by digital fluorescence microscopy. Results are shown as mean  $\pm$  SEM of 4 independent experiments with at least 8 observations.

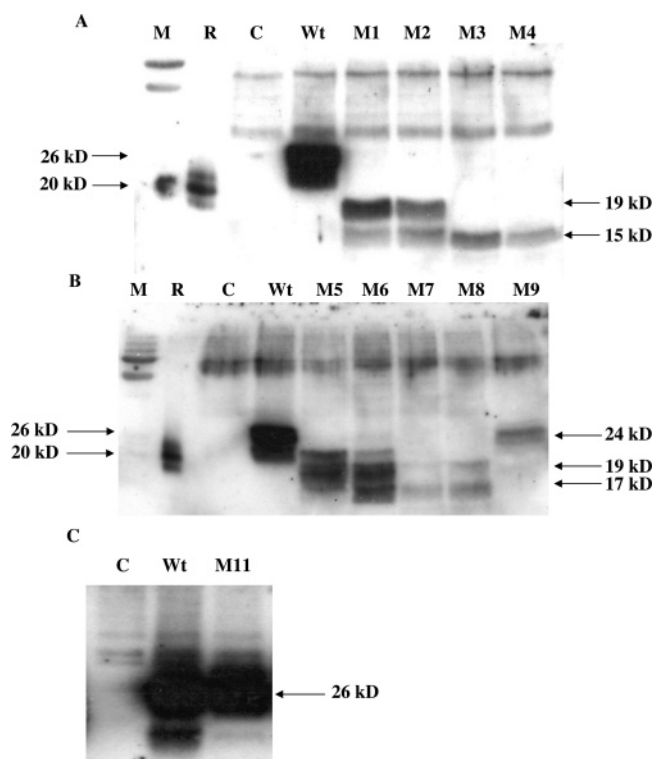


FIGURE 3: Protein levels of PANDER mutants expressed in  $\beta$ -TC3 cells. PANDER mutants were expressed in  $\beta$ -TC3 cells as described in Figure 2 and Materials and Methods, followed by Western blot analysis (20  $\mu$ g of protein/lane) with an anti-PANDER antibody. (A) Western blot of control, Wt, and C-terminal truncated PANDERS (M1 to M4) expressed in  $\beta$ -TC3 cells. (B) Western blot of control, Wt, and N-terminal truncated PANDERS (M5 to M9) expressed in  $\beta$ -TC3 cells. (C) Western blot of M11 expressed in  $\beta$ -TC3 cells. M, molecular weight ladder; R, recombinant PANDER protein; C, control cells transfected with empty pShuttle vector. Results are representative of at least 3 independent experiments.

all the activity of wild-type PANDER ( $91 \pm 6\%$ , Figure 4C,D). This strongly indicates that the N-terminus of

PANDER, including helix A and the first two cysteines, C63 and C69, is not important for the cytotoxic activity of PANDER. M6 without Cys91 maintained only  $50 \pm 4\%$  activity ( $p < 0.05$  when compared to Wt and M5, Figure 4C,D). This shows that the third cysteine, C91, is important for PANDER's function. Taking together, it seems that the third and fourth cysteines, C91 and C229, form one disulfide bond in wild-type PANDER and this disulfide bond is important for function. The fact that M5 was almost fully active is consistent with our previous reports that recombinant PANDER with its N-terminus truncated is as effective as full length PANDER (27). M7 and M8 maintained about  $38 \pm 7\%$  and  $53 \pm 10\%$  activity, showing that helix B is important. M8 maintained more activity than M7, indicating that insertion of a cysteine at the N-terminus of M7 restored some activity and that C229 may form a disulfide bond with C91. M9 maintained  $53 \pm 13\%$  activity, also confirming that helix B is important for cytotoxic function (Figure 4C,D). M11 with a single mutation of C229 to serine maintained cytotoxic activity similar to that of M6 ( $52 \pm 11\%$  versus  $53 \pm 4\%$ ), while M5 maintained most of Wt PANDER activity ( $86 \pm 4\%$ ) (Figure 4E,F), further confirming that C91 and C229 do form one disulfide bond. In summary, helices B and C are essential for the cytotoxic activity of PANDER, while the N-terminus is not required.

**Effect of Mutant PANDERS on Insulin Release and Acute Insulin Secretion of  $\beta$ -TC3 Cells.** Impaired insulin release was observed in M1 ( $75 \pm 3\%$  of vehicle control) and M2 ( $76 \pm 3.0\%$ ) (Figure 5A) expressing cells, which, however, was not different from the impaired insulin release observed with Wt PANDER ( $73 \pm 2\%$ ). In contrast, M3 ( $94 \pm 7.0\%$ ) and M4 ( $89 \pm 5\%$ ) did not affect insulin release significantly. In the case of the PANDER mutants with N-terminus truncations, M5 ( $57 \pm 6\%$ ) and M6 ( $69 \pm 5\%$ ) impaired insulin release significantly, which was not different from Wt PANDER ( $67 \pm 4\%$ ). M7 ( $90 \pm 9\%$ ), M8 ( $87 \pm 15\%$ ),

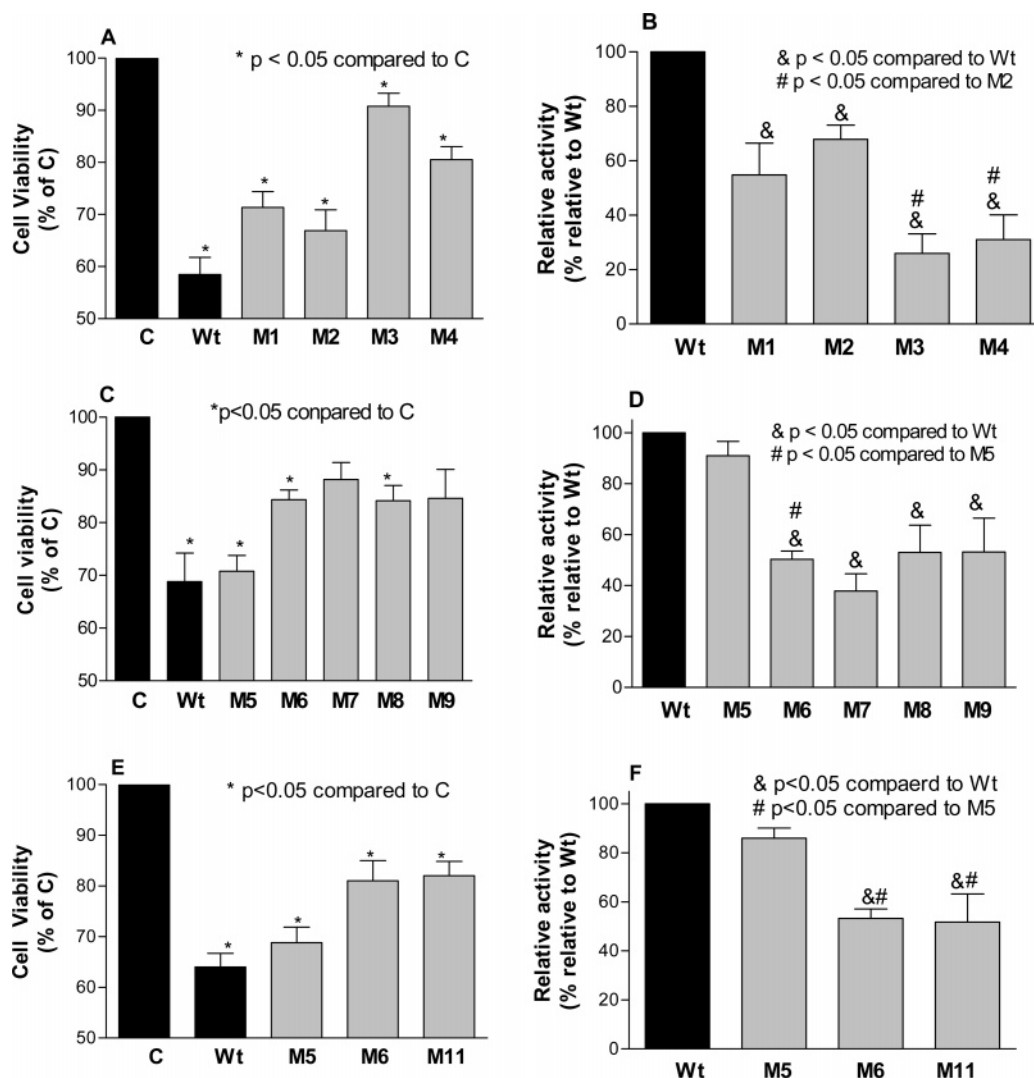


FIGURE 4: Effect of PANDER mutants on  $\beta$ -TC3 cell viability.  $\beta$ -TC3 cells were seeded ( $3.0 \times 10^5$  per well) and transfected with PANDER mutants as described in Materials and Methods. Cell viability was measured with the MTT assay. Results are expressed as cell viability (% of control) as well as relative activity (% relative to wild-type PANDER), which was calculated as described in Materials and Methods. (A) Cell viability assay of control, Wt, and C-terminal truncated PANDERS. (B) Relative activity of C-terminal truncated PANDERS. (C) Cell viability assay of control, Wt, and N-terminal truncation PANDERS. (D) Relative activity of Wt and N-terminal truncation PANDERS. (E) Cell viability assay of control, Wt, M6, and M11 PANDERS. (F) Relative activity of M6 and M11 PANDERS. Results are shown as mean  $\pm$  SEM of at least 15 observations from at least 5 independent experiments. \*,  $P < 0.05$  compared to control (C); &,  $P < 0.05$  compared to wild-type (Wt); #,  $P < 0.05$  compared to M2 or M5.

and M9 ( $96 \pm 7\%$ ) did not affect insulin release significantly, though M8 and M9 maintained about 50% of cytotoxic activity compared to Wt PANDER (Figure 5B). M11 also impaired insulin release significantly, which was  $72 \pm 3\%$  of control and not different from Wt PANDER ( $68 \pm 4\%$ , Figure 5C). Similarly to insulin release, impaired acute insulin secretion was observed with M1 ( $74 \pm 4\%$ ), M2 ( $76 \pm 5\%$ ), M5 ( $64 \pm 6\%$ ), M6 ( $74 \pm 5\%$ ), and M11 ( $76 \pm 5\%$ ) PANDERS, which were not significantly different from Wt PANDER ( $65 \pm 3\%$ ). The results also indicated that M5 was as effective as Wt, while M1, M2, M6, and M11 were slightly less effective than Wt and M5 (Figure 5D). In contrast, M3 ( $83 \pm 5\%$ ), M4 ( $92 \pm 8\%$ ), M7 ( $87 \pm 7\%$ ), M8 ( $86 \pm 8\%$ ), and M9 ( $94 \pm 5\%$ ) did not affect acute insulin secretion significantly (Figure 5E). However, no significant difference was detected in acute insulin secretion if the amount of insulin secreted was normalized to number of live cells (data not shown). This implies that PANDER impairs insulin secretion by killing the cells but does not

affect insulin secretion ability of live cells.

**Calcein-AM/EthD-1 Fluorescence Assay of Mutant PANDER.** Calcein-AM stains the cytosol of live cells, and EthD-1 stains the nuclei of dead cells. Almost no dead cells were observed in control cells transfected with pShuttle, while a large number of dead cells were recorded among cells transfected with Wt, M1, M2, M5, and M6 (Figure 6A). Quantitation of the amount of green fluorescence emitted by live cells showed that Wt and M5 transfected cells were  $56 \pm 3\%$  and  $52 \pm 5\%$  of the vehicle control, indicating that M5 was fully active as expected from the cytotoxicity data. Fluorescence of M1, M2, and M6 was  $67 \pm 4\%$ ,  $69 \pm 10\%$ , and  $66 \pm 3\%$  of the vehicle control, indicating that they are slightly less active than Wt and M5 (Figure 6B).

**Effects of Ad-Truncated PANDER on  $\beta$ -TC3 Cells.** Ad-PANDER was used to overcome the limitation of low efficiency for plasmid transfection in  $\beta$ -TC3 cells. Ad-M1, Ad-M2, Ad-M3, and Ad-M4 PANDERS were constructed and used to infect  $\beta$ -TC3 cells. Quantitative RT-PCR (Figure

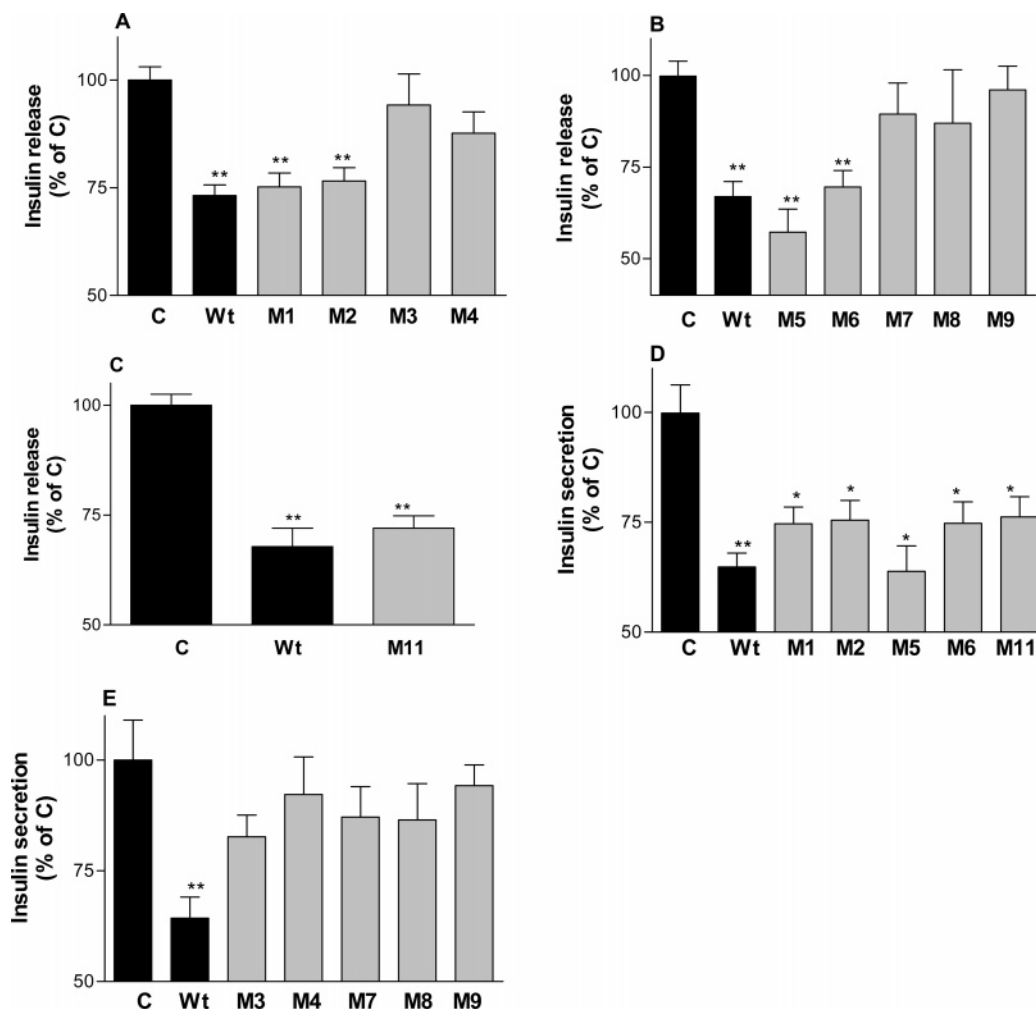


FIGURE 5: Effect of PANDER mutants on insulin release and acute insulin secretion from  $\beta$ -TC3 cells. See Figure 4 and Materials and Methods for experimental details. Results are shown as mean  $\pm$  SEM of insulin release and insulin secretion (normalized to control) of at least 15 observations from at least 5 independent experiments. \*,  $P < 0.05$ , \*\*,  $P < 0.01$  compared to control (C).

7A) and Western blot assay (Figure 7B) showed that the minimal dose of Ad-PANDER for overexpression was 500 particles/cell. MTT assays (data not shown) indicated that a dose of 5000 particles/cell was required for cell death. The same dose of Ad-GFP was used as negative control. Ad-M1 maintained about  $58 \pm 6\%$  activity, while Ad-M2 maintained about  $50 \pm 6\%$  activity. Ad-M3 and Ad-M4 maintained about  $38 \pm 2\%$  and  $27 \pm 19\%$  activity (Figure 8A,B); these results are consistent with the transfection studies.

**Role of PANDER Signal Peptide in  $\beta$ -TC3 Cells.** M10 plasmid was constructed with the entire signal peptide (aa 2–29) deleted except for Met1 (ATG) (Figure 1). Transfection of  $\beta$ -TC3 cells with M10 did not produce the corresponding M10 protein in the cells, although real time RT-PCR showed that M10 could be effectively transcribed (Figure 9A,B). MTT assay indicated that M10-PANDER did not kill cells (Figure 9C), which is due to the lack of M10 protein translation.

The culture medium of  $\beta$ -TC3 cells transfected with Wt PANDER was collected and concentrated with ammonium sulfate. Western blotting experiments indicated that two secreted PANDER isoforms were detected with masses of 23 and 26 kDa (Figure 9B). The 23 kDa isoform was far more abundant than the 26 kDa one in the medium. In cell lysates, however, the 26 kDa product was more abundant

(Figure 9B). Our recombinant PANDER consists of two isoforms of 20 and 21 kDa, respectively (26). Hence, the main PANDER isoform in cell lysate was the full-length protein of 26 kDa (235 amino acids), while the secreted PANDER isoform probably had the signal peptide cleaved generating a 22.6 kDa product (aa 30–235).

## DISCUSSION

PANDER is a 235 amino acid protein with 4 helices, 2 putative disulfide bonds, and a secretion signal peptide, present in  $\alpha$ - and  $\beta$ -cells of mouse, rat, and human pancreatic islets (26, 27). There are several cleavage products of PANDER, which include several N-terminus truncated proteins (26). Our previous studies showed that this mixture of recombinant PANDER products has potent cytotoxic effects on  $\alpha$ - and  $\beta$ -cells of mouse, rat, and human pancreatic islets (27). However, the underlying mechanism of PANDER-induced cytotoxicity as well as the identity of the PANDER receptor remains unclear. Identification of the PANDER receptor is very important in order to further elucidate PANDER's physiological role(s). As a first step toward that goal, in this study, we have identified the region of PANDER which confers  $\beta$ -cell cytotoxicity. A series of truncated and mutated PANDER analogues were constructed and expressed in  $\beta$ -TC3 cells in order to determine the structure–function



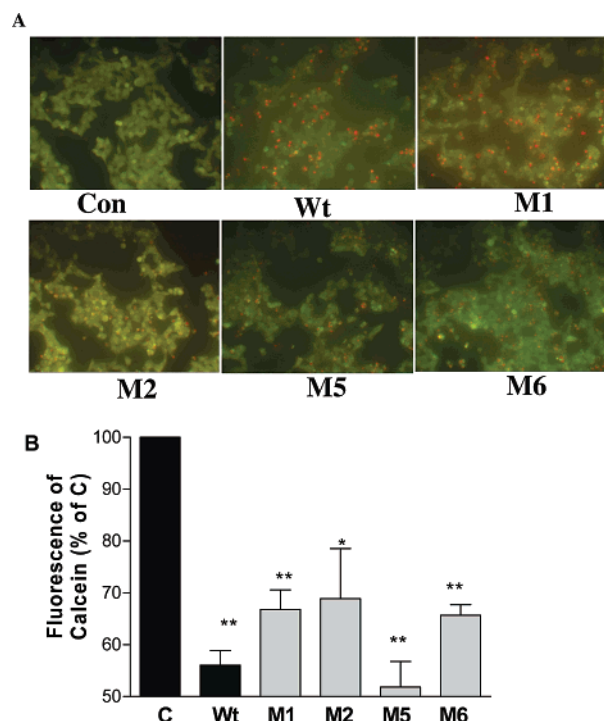


FIGURE 6: Live/dead assay of  $\beta$ -TC3 cells transfected with Wt and PANDER mutants.  $\beta$ -TC3 cells were transfected with PANDER mutants as described in Materials and Methods. Cells were stained with 10 nM calcein-AM and 4  $\mu$ M EthD-1 at room temperature for 45 min. Images of the stained cells were captured with digital fluorescence microscopy using SimplePCI software. (A) Representative fields of  $\beta$ -TC3 cells stained with calcein-AM (green) and EthD-1 (red). (B) Quantitation of calcein fluorescence of live cells normalized to control. Results are shown as mean  $\pm$  SEM of at least 9 observations from 3 independent experiments. \*,  $P < 0.05$ , \*\*,  $P < 0.01$  compared to control.

relationship of PANDER. The relative activities of these PANDER mutants were compared to that of Wt-PANDER using  $\beta$ -cell death and insulin secretion assays.

Deletion of helix D alone causes a 40–50% loss of PANDER's cytotoxic activity (Figure 4A,B), while truncation of both helix C and helix D results in a nearly total loss of cytotoxic activity. Insulin secretion and calcein-AM assays also indicated that deletion of helix D (mutants M1 and M2) maintained most activity (Figures 4A,B, 5A–E, and 6A,B), while deletion of both helices C and D (M3 and M4) conferred the greatest loss of activity (Figures 4A,B and 5A,E). Thus helix C is vital for PANDER activity, while helix D may be important, but not vital. Mutation of the third cysteine (C91) to a serine (M6) or the fourth cysteine (C229) to a serine (M11) decreased PANDER's cytotoxic activity by approximately half, and M6 and M11 maintain similar activity in both cell viability and insulin secretion assays (Figures 4E,F and 5D). Thus, the third and fourth cysteines form a disulfide bond that is important for function (Figures 4C–F and 5D). Because mutant M5 (truncation of the N-terminus including helix A, and most of the loop between helices A and B) did not lose activity in any of the assays (Figures 4C–F, 5B,D, and 6), neither helix A nor the first and second cysteines (63 and 69) in the AB loop are required for PANDER cytotoxicity.

The cell viability and insulin secretion assay indicated that mutants M7 and M8 lost most of their activity. Thus, helix B may be vital for function. To further test the role of helix

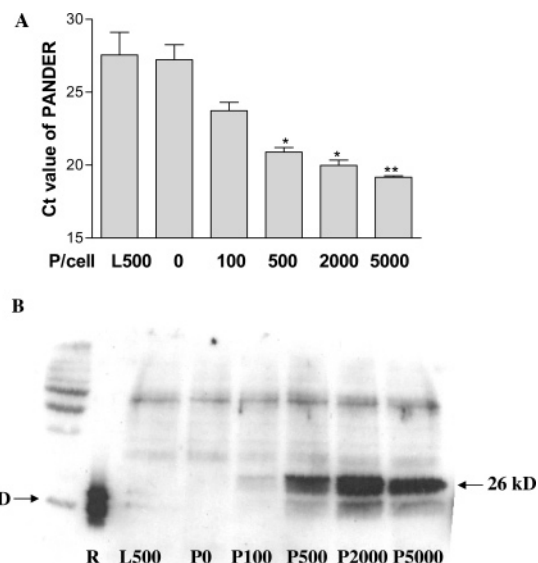


FIGURE 7: Infection of  $\beta$ -TC3 cells with Ad-PANDERs. One day before infection,  $6.0 \times 10^5$   $\beta$ -TC3 cells were seeded in 12-well plates in 1 mL of normal RPMI 1640 (10% FBS, 3 mM glucose). Cells were washed twice with 1 mL of serum-free RPMI 1640. Serum-free medium (250  $\mu$ L) and virus were added to each well to reach the indicated final concentration (particles/cell). (A) Real-time RT-PCR PANDER analysis expressed as mean  $\pm$  SEM. \*,  $P < 0.05$ , \*\*,  $P < 0.01$  compared to control infection. (B) PANDER Western blotting. L, Ad-LacZ; P, Ad-PANDER; R, recombinant PANDER protein. Results are representative of 4 independent experiments in duplicate.

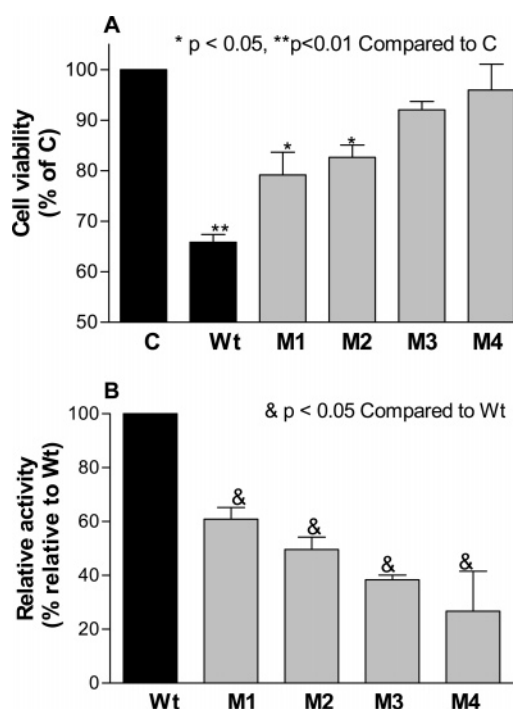


FIGURE 8: Effect of Wt and mutant Ad-PANDERs on  $\beta$ -TC3 cell viability.  $\beta$ -TC3 cells were infected in 24-well plates with 5000 virus particles/cell and cultured for 2 days. MTT assay was performed as described in Materials and Methods and the data normalized to control (cells infected with Ad-GFP). (A) Viability of  $\beta$ -TC3 cells infected with Wt and mutant PANDER adenoviruses. (B) Relative activity of PANDER mutants. Results are shown as mean  $\pm$  SEM of at least 12 observations from 4 independent experiments. \*,  $P < 0.05$ , \*\*,  $P < 0.01$  compared to control; &,  $P < 0.05$  compared to Wt.



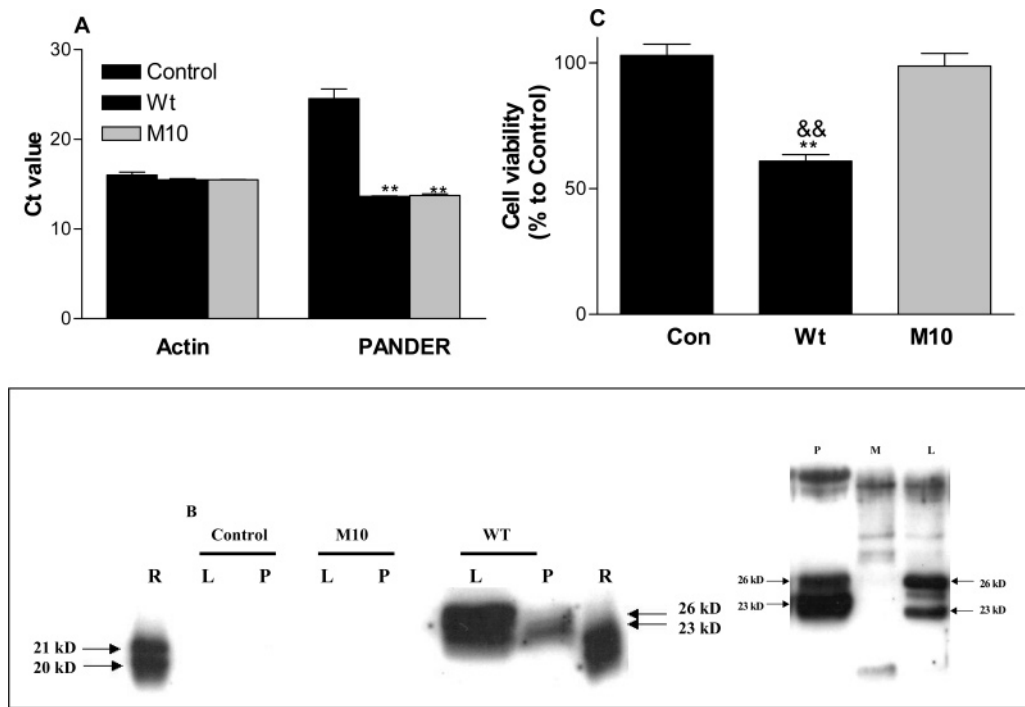


FIGURE 9: Effect of PANDER mutant with no signal peptide on  $\beta$ -TC3 cell viability. (A) Real time RT-PCR. (B) Secretion of PANDER protein.  $\beta$ -TC3 cells were transfected and cultured for 48 h. Medium and lysate samples were analyzed by Western blot as described in Materials and Methods. Control, empty pShuttle vector; M10, M10-PANDER; WT, Wt-PANDER; R, recombinant PANDER protein; P, 25  $\mu$ L/lane of precipitated medium; L, 5  $\mu$ g/lane of cell lysate; M, molecular weight ladder. (C) MTT assay. Results are representative of four independent experiments with more than 12 observations. \*\*,  $P < 0.01$  compared to control; &&,  $P < 0.01$  compared to M10.

B, we constructed a mutant M9 without helix B but maintaining helix A, the loop between helices A and B loop and the first two cysteines. M9 maintained about 50% cytotoxic activity and did not affect insulin secretion significantly. Thus, helix B is vital for function. As suggested by the experiments with mutant M5, the results with mutant M9 confirm that helix A and most of the AB loop are not needed for function.

Based on our studies, we suggest that the region between Cys91 and Phe152 (helices B and C) and the Cys91–C229 disulfide bond are functionally important for PANDER cytotoxicity. The role of four cysteines in PANDER's biologic activity is very similar to that found in human IL-6. The four cysteines of human IL-6 form two disulfide bonds, and the first one (Cys45–Cys51) is not important, while the second one (Cys74–Cys84) is necessary for its function and receptor binding, which is likely to anchor the receptor binding portion of the AB loop to helix B (32). Another report indicated that a mutant human IL-6 lacking the 22-residues at its N-terminus and with mutations of Cys45 and Cys51 to serine maintained most of wild-type IL-6 activity, which is very similar to M5-PANDER observed in this study (33), suggesting that the Cys91–Cys229 disulfide bond of PANDER might be involved in receptor binding. We anticipate that the identification of this crucial region and disulfide bond of PANDER will be useful to guide our future experiments aimed at identifying the receptor of PANDER (Figure 10).

Although mutant PANDERs were detected in cell lysates (Figure 3A,B), secreted PANDER analogues were not detected in the media of cells transfected with M1, M2, M5, and M6 (data not shown). In addition to the PANDER protein with the expected molecular weight, a smaller PANDER

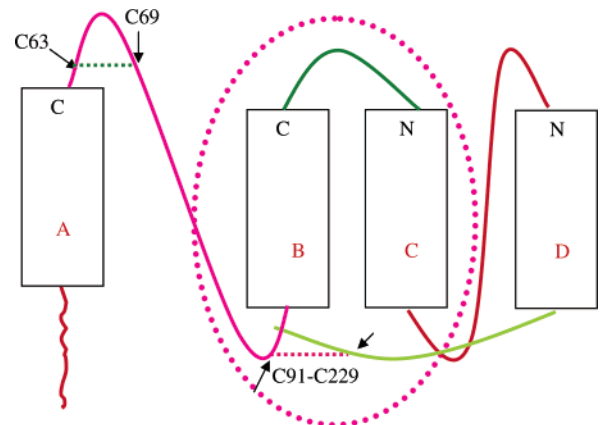


FIGURE 10: Identification of the essential domain of PANDER conferring  $\beta$ -cell cytotoxicity. Waved line is the signal peptide of PANDER; A, B, C, and D are the four helices of PANDER; C63, C69, C91, and C229 are the four cysteines in PANDER while the disulfide bonds are indicated by the dashed line. The essential active domain of PANDER is circled.

analogue was also detected in these cell lysates (Figure 3A,B). We postulate that this analogue has no signal peptide because its size is smaller than expected and matches the predicted size of PANDER without the signal peptide (Figure 3,B). This also implies that the signal peptide of M1, M2, M5, and M6 can be cleaved successfully. Hence, failure to detect secreted truncated PANDERs in the medium of overexpressing cells is probably due to the following: (1) Correct structure and conformation, which are important for PANDER secretion, have been compromised in the PANDER mutants, which may affect their ability to be packaged into secretory granules. Preliminary data indicate that PANDER can be packaged into the insulin secretory granules and is secreted in response to glucose (unpublished observa-

tions). (2) Stability of the mutant PANDERs is decreased due to large-scale truncation. (3) Our current antibodies recognize the truncated PANDERs at a lower affinity than Wt PANDER (Figure 3A,B). (4) Mutant PANDER levels in the medium may be too low for detection.

As previously described, PANDER causes  $\beta$ -cell death via apoptosis (27). We hypothesize that PANDER may activate the apoptotic pathway through two different mechanisms. The first mechanism would imply the existence of a membrane receptor which would explain how secreted PANDER or exogenous recombinant PANDER (27) causes  $\beta$ -cell death. The overexpression of PANDER in the  $\beta$ -TC3 cells reduced the cell viability by about 50% (Figures 4 and 6) even though the transfection efficiency was only about 20–40% (Figure 3B). This suggests that PANDER or other molecules released from dying cells will also kill nearby cells. Furthermore, Western blot analysis showed that the full-length PANDER could be detected in the medium (Figure 9B). A second mechanism would invoke the presence of an intracellular soluble PANDER receptor. Many cytokines, including TNF- $\alpha$ , IL-2, IFN- $\gamma$ , and leptin, bind to soluble receptors that are intracellular or in the circulation system (34–39). The fact that M1, M2, M6, and M5 (which is as effective as wild-type PANDER) maintain most of PANDER's activity but are not released supports the latter mechanism.

PANDER may have different roles depending on its concentration and target tissue(s). So far, we have shown that exogenous PANDER and overexpressed PANDER cause  $\beta$ -cell apoptosis. In addition, the proinflammatory cytokine interferon- $\gamma$  stimulates PANDER expression in  $\beta$ -cells (27, 28, 40). These in vitro results are consistent with a role of PANDER in the destruction of the  $\beta$ -cell. However, since recombinant PANDER also causes  $\alpha$ -cell apoptosis in vitro (27), the role of PANDER in the pathogenesis of type 1 diabetes is unclear. We have now shown that the PANDER promoter has a robust glucose response, and that PANDER is cosecreted with insulin in response to glucose (41, 42), suggesting that PANDER may also have an additional role in glucose homeostasis.

In conclusion, our studies have shown that the region between Cys91 and Phe152, which corresponds to helices B and C, and the second disulfide bond between Cys91 and Cys229, which likely anchor the receptor binding portion(s) located within helix B, and/or helix C, and/or the BC loop together, are required for PANDER's cytotoxic effects on  $\beta$ -cells.

## REFERENCES

- Mordes, J. P., Bortell, R., Blankenhorn, E. P., Rossini, A. A., and Greiner, D. L. (2004) Rat models of type 1 diabetes: genetics, environment, and autoimmunity, *ILAR J.* 45, 278–291.
- Bach, J.-F. (1994) Insulin-dependent diabetes mellitus as an autoimmune disease, *Endocr. Rev.* 15, 516–542.
- Atkinson, M. A., and Eisenbarth, G. S. (2001) Type 1 diabetes: new perspectives on disease pathogenesis and treatment, *Lancet* 358, 221–229.
- Mauricio, D., and Mandrup-Poulsen, T. (1998) Apoptosis and the pathogenesis of IDDM: a question of life and death, *Diabetes* 47, 1537–1543.
- Nerup, J., Mandrup-Poulsen, T., Helqvist, S., Andersen, H. U., Pociot, F., Reimers, J. I., Cuartero, B. G., Karlens, A. E., Bjerre, U., and Lorenzen, T. (1994) On the pathogenesis of IDDM, *Diabetologia* 37 (Suppl. 2), S82–S89.
- Rabinovitch, A., and Suarez-Pinzon, W. L. (1998) Cytokines and their roles in pancreatic islet beta-cell destruction and insulin-dependent diabetes mellitus, *Biochem. Pharmacol.* 55, 1139–1149.
- Major, C. D., and Wolf, B. A. (2001) Interleukin-1 $\beta$  stimulation of c-Jun NH(2)-terminal kinase activity in insulin-secreting cells: evidence for cytoplasmic restriction, *Diabetes* 50, 2721–2728.
- Kutlu, B., Darville, M. I., Cardozo, A. K., and Eizirik, D. L. (2003) Molecular regulation of monocyte chemoattractant protein-1 expression in pancreatic beta-cells, *Diabetes* 52, 348–355.
- Chang, I., Cho, N., Kim, S., Kim, J. Y., Kim, E., Woo, J. E., Nam, J. H., Kim, S. J., and Lee, M. S. (2004) Role of Calcium in Pancreatic Islet Cell Death by IFN- $\gamma$ /TNF- $\alpha$ , *J. Immunol.* 172, 7008–7014.
- Lacy, P. E. (1994) The intraislet macrophage and type I diabetes, *Mt. Sinai J. Med.* 61, 170–174.
- Peterson, D. A., Lucidi-Phillipi, C. A., Murphy, D. P., Ray, J., and Gage, F. H. (1996) Fibroblast growth factor-2 protects entorhinal layer II glutamatergic neurons from axotomy-induced death, *J. Neurosci.* 16, 886–898.
- Bergman, B., and Haskins, K. (1997) Autoreactive T-cell clones from the nonobese diabetic mouse, *Proc. Soc. Exp. Biol. Med.* 214, 41–48.
- Toyoda, H., and Formby, B. (1998) Contribution of T cells to the development of autoimmune diabetes in the NOD mouse model, *BioEssays* 20, 750–757.
- Arnush, M., Scarim, A. L., Heitmeier, M. R., Kelly, C. B., and Corbett, J. A. (1998) Potential role of resident islet macrophage activation in the initiation of autoimmune diabetes, *J. Immunol.* 160, 2684–2691.
- Borst, S. E. (2004) The role of TNF- $\alpha$  in insulin resistance, *Endocrine* 23, 177–182.
- Silha, J. V., Krsek, M., Skrha, J., Sucharda, P., Nyomba, B. L. G., and Murphy, L. J. (2004) Plasma resistin, leptin and adiponectin levels in non-diabetic and diabetic obese subjects, *Diabetic Med.* 21, 497–499.
- Stejskal, D., Lacnak, B., Hamplova, A., Proskova, J., Horalik, D., Adamovska, S., and Jurakova, R. (2003) Resistin - determination in persons with diabetes mellitus of Type 2 or in individuals with acute inflammatory disease, *Diabetologia* 46, A384.
- McTernan, P. G., Fisher, F. M., Valsamakis, G., Chetty, R., Harte, A., McTernan, C. L., Clark, P. M. S., Smith, S. A., Barnett, A. H., and Kumar, S. (2003) Resistin and type 2 diabetes: Regulation of resistin expression by insulin and rosiglitazone and the effects of recombinant resistin on lipid and glucose metabolism in human differentiated adipocytes, *J. Clin. Endocrinol. Metab.* 88, 6098–6106.
- Scheen, A. J. (2003) Current management strategies for coexisting diabetes mellitus and obesity, *Drugs* 63, 1165–1184.
- Mandrup-Poulsen, T. (2003) Beta cell death and protection, *Ann. N.Y. Acad. Sci.* 1005, 32–42.
- Eizirik, D. L., and Darville, M. I. (2001) Beta-cell apoptosis and defense mechanisms: lessons from type 1 diabetes, *Diabetes* 50 (Suppl. 1), S64–S69.
- Sarvetnick, N., Liggitt, D., Pitts, S. L., Hansen, S. E., and Stewart, T. A. (1988) Insulin-dependent diabetes mellitus induced in transgenic mice by ectopic expression of class II MHC and interferon- $\gamma$ , *Cell* 52, 773–782.
- Stewart, A. G., Tomlinson, P. R., and Wilson, J. (1993) Airway wall remodelling in asthma: A novel target for the development of anti-asthma drugs, *Trends Pharmacol. Sci.* 14, 275–279.
- Picarella, D. E., Kratz, A., Li, C., Ruddell, N. H., and Flavell, R. A. (1993) Transgenic tumor necrosis factor (TNF)- $\alpha$  production in pancreatic islets leads to insulinitis, not diabetes: Distinct patterns of inflammation in TNF- $\alpha$  and TNF- $\beta$  transgenic mice, *J. Immunol.* 150, 4136–4150.
- Aurora, R., and Rose, G. D. (1998) Seeking an ancient enzyme in *Methanococcus jannaschii* using ORF, a program based on predicted secondary structure comparisons, *Proc. Natl. Acad. Sci. U.S.A.* 95, 2818–2823.
- Zhu, Y., Xu, G., Patel, A., McLaughlin, M. M., Silverman, C., Knecht, K., Sweitzer, S., Li, X., McDonnell, P., Mirabile, R., Zimmerman, D., Boyce, R., Tierney, L. A., Hu, E., Livi, G. P., Wolf, B., Abdel-Meguid, S. S., Rose, G. D., Aurora, R., Hensley, P., Briggs, M., and Young, P. R. (2002) Cloning, expression, and initial characterization of a novel cytokine-like gene family, *Genomics* 80, 144–150.

27. Cao, X., Gao, Z., Robert, C. E., Greene, S., Xu, G., Xu, W., Bell, E., Campbell, D., Zhu, Y., Young, R., Trucco, M., Markmann, J. F., Naji, A., and Wolf, B. A. (2003) Pancreatic-Derived Factor (FAM3B), a Novel Islet Cytokine, Induces Apoptosis of Insulin-Secreting beta-Cells, *Diabetes* 52, 2296–2303.
28. Cao, X., Yang, J., Burkhardt, B., Gao, Z., Wong, R. K., Greene, S., Wu, J., and Wolf, B. A. (2005) Effects of over-expression of Pancreatic-Derived Factor (FAM3B) in isolated mouse islets and insulin-secreting Beta-TC3 cells. *Am. J. Physiol.* (in press).
29. Fitzhugh, D. J., Naik, S., Caughman, S. W., and Hwang, S. T. (2000) Cutting edge: C-C chemokine receptor 6 is essential for arrest of a subset of memory T cells on activated dermal microvascular endothelial cells under physiologic flow conditions in vitro, *J. Immunol.* 165, 6677–6681.
30. Yang, J., Wong, R. K., Wang, X., Moibi, J., Hessner, M. J., Greene, S., Wu, J., Sukumvanich, S., Wolf, B. A., and Gao, Z. (2004) Leucine Culture Reveals That ATP Synthase Functions as a Fuel Sensor in Pancreatic {beta}-Cells, *J. Biol. Chem.* 279, 53915–53923.
31. Bell, E., Cao, X., Moibi, J. A., Greene, S. R., Young, R., Trucco, M., Gao, Z., Matschinsky, F. M., Deng, S., Markman, J. F., Naji, A., and Wolf, B. A. (2003) Rapamycin Has a Deleterious Effect on MIN-6 Cells and Rat and Human Islets, *Diabetes* 52, 2731–2739.
32. Snouwaert, J. N., Leebeek, F. W., and Fowlkes, D. M. (1991) Role of disulfide bonds in biologic activity of human interleukin-6, *J. Biol. Chem.* 266, 23097–23102.
33. Breton, J., La, F. A., Bertolero, F., Orsini, G., Valsasina, B., Ziliotto, R., De, F., V., Polverino de, L. P., and Fontana, A. (1995) Structure, stability and biological properties of a N-terminally truncated form of recombinant human interleukin-6 containing a single disulfide bond, *Eur. J. Biochem.* 227, 573–581.
34. Bencsath, M., Blaskovits, A., and Borvendeg, J. (2003) Biomolecular cytokine therapy, *Pathol. Oncol. Res.* 9, 24–29.
35. Fernandez-Real, J. M. and Ricart, W. (1999) Insulin resistance and inflammation in an evolutionary perspective: the contribution of cytokine genotype/phenotype to thriftiness, *Diabetologia* 42, 1367–1374.
36. Kotenko, S. V., and Langer, J. A. (2004) Full house: 12 receptors for 27 cytokines, *Int. Immunopharmacol.* 4, 593–608.
37. Kwan, T. S., Padrines, M., Theoleyre, S., Heymann, D., and Fortun, Y. (2004) IL-6, RANKL, TNF-alpha/IL-1: interrelations in bone resorption pathophysiology, *Cytokine Growth Factor Rev.* 15, 49–60.
38. Levine, S. J. (2004) Mechanisms of soluble cytokine receptor generation, *J. Immunol.* 173, 5343–5348.
39. Walter, M. R. (2002) Crystal structures of alpha-helical cytokine-receptor complexes: we've only scratched the surface, *BioTechniques Suppl.*, 46–47.
40. Xu, W., Gao, Z., Wu, J., and Wolf, B. A. (2005) Interferon- $\gamma$ -induced Regulation of the Pancreatic Derived Cytokine FAM3B in Islets and Insulin-secreting  $\beta$ TC3 Cells, *Mol. Cell. Endocrinol.* (in press).
41. Burkhardt, B. R., Yang, M. C., Robert, C. E., Yang, J., Greene, S. R., McFadden, K., Gao, Z. Y., and Wolf, B. A. (2005) Islet cell-line specific and glucose-responsive expression of the PANDER promoter, *Biochim. Biophys. Acta* (in press).
42. Yang, J., Young, R. A., Robert, C., Burkhardt, B., Wu, J., Gao, Z., and Wolf, B. A. (2005) Mechanisms of glucose-induced secretion of PANDER in pancreatic beta cells, *Diabetes* 54 (Suppl. 1), A646.

BI0503908